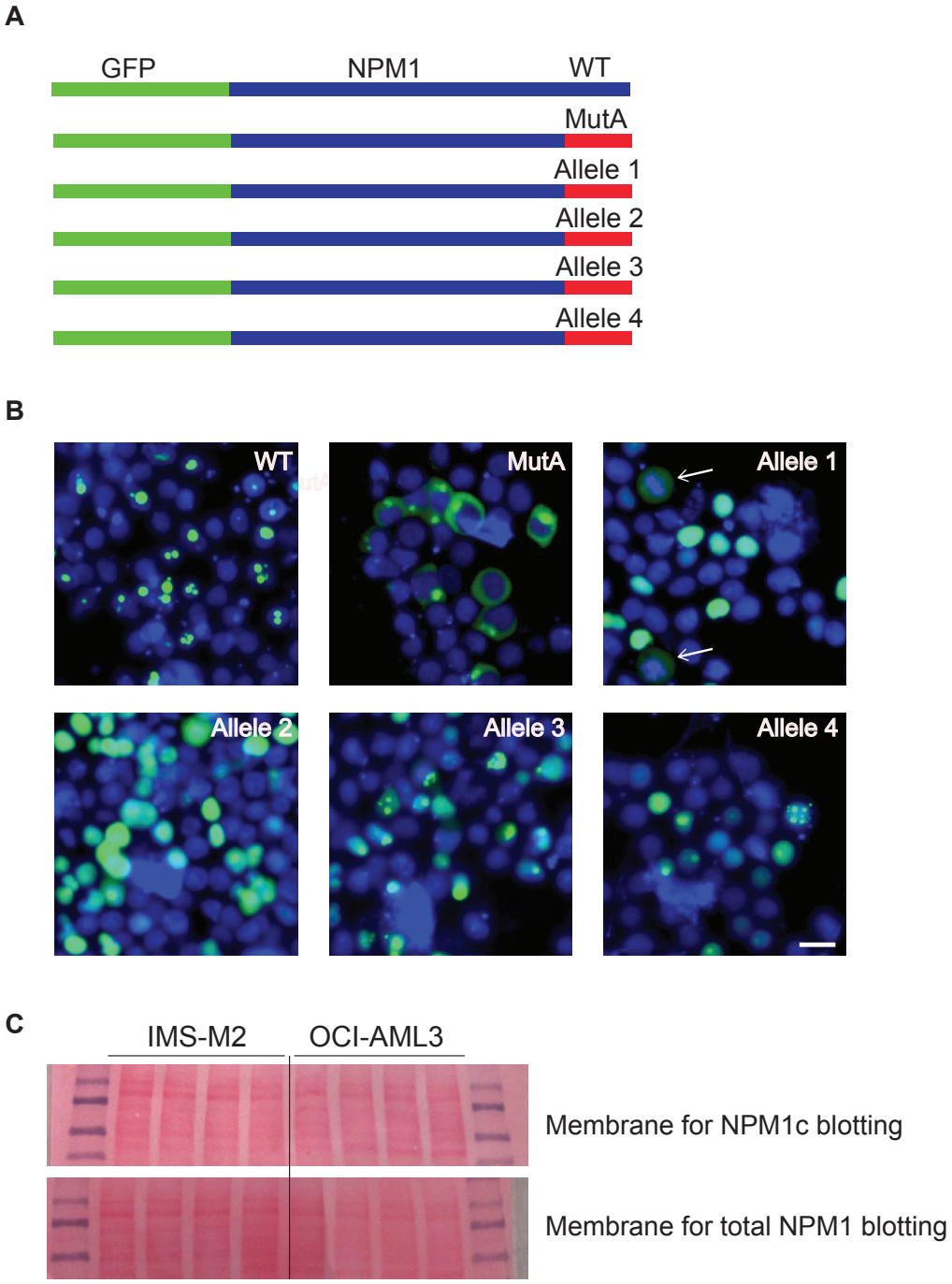

Figure S1. Validation of NPM1c nuclear relocalization (Related to Figure 1).

(A) Schematic representation of the alleles cloned into pEGFP-C1-NPM1 plasmid. GFP is fused at the N-terminus of the NPM1 protein.

(B) Fluorescence microscopy of 293T cells transfected with GFP-NPM1 alleles shown in (A). White arrows indicate mitoses. Scale bar 20μm.

(C) Ponceau staining of western blot membranes used in Figure 1D.

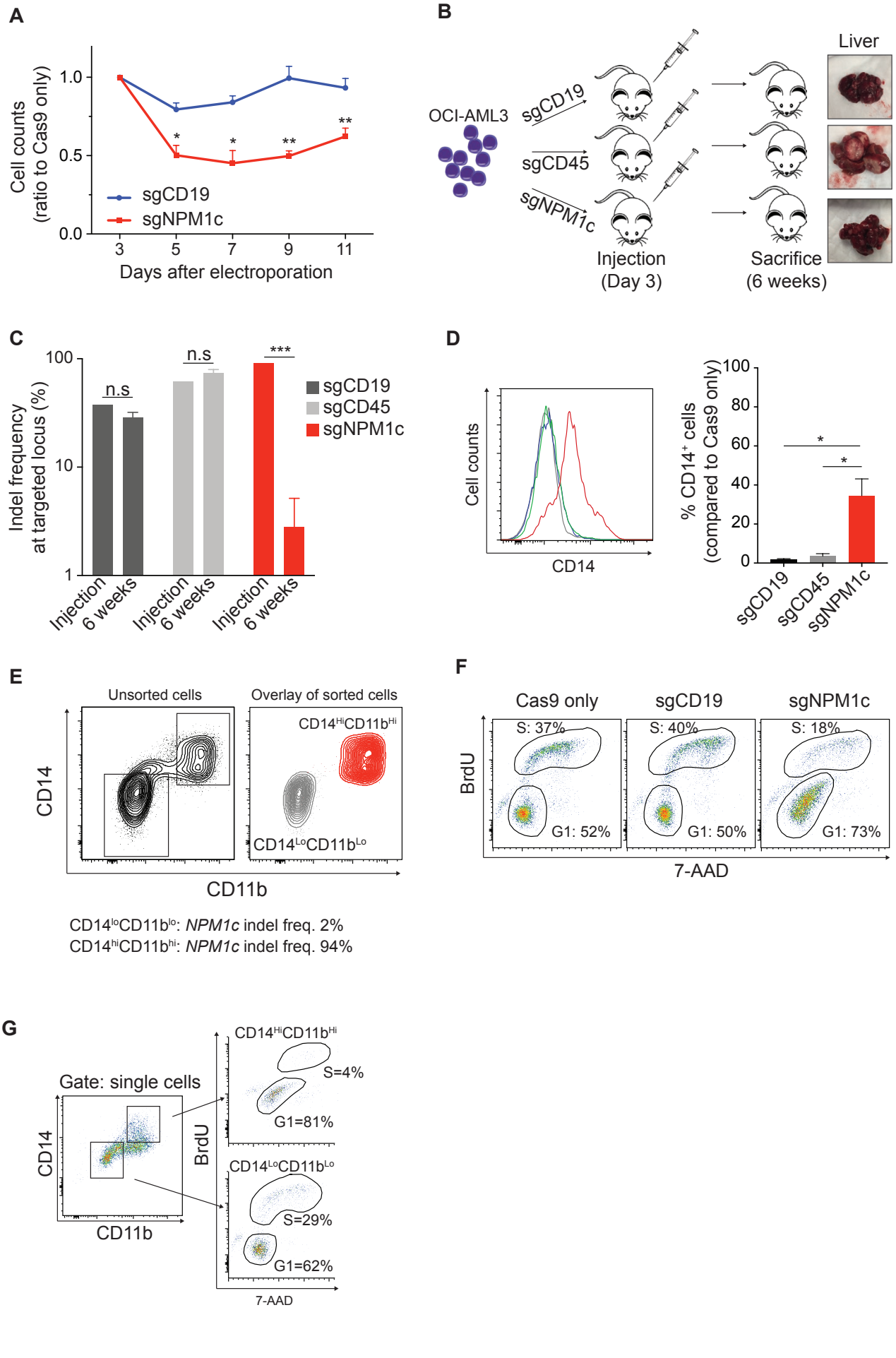
A
Cell counts (ratio to Cas9 only)
1.0
0.5
0.0
3
5
7
9
11
Days after electroporation
sgCD19
sgNPM1c
*
*
**
**
B
OCI-AML3
sgCD19
sgCD45
sgNPM1c
Injection (Day 3)
Sacrifice (6 weeks)
Liver
C
Indel frequency at targeted locus (%)
100
10
1
n.s
n.s
***
sgCD19
sgCD45
sgNPM1c
Injection
6 weeks
D
Cell counts
CD14
% CD14+ cells (compared to Cas9 only)
100
80
60
40
20
0
*
*
sgCD19
sgCD45
sgNPM1c
E
Unsorted cells
Overlay of sorted cells
CD14
CD11b
CD14HiCD11bHi
CD14LoCD11bLo
CD14loCD11blo: NPM1c indel freq. 2%
CD14hiCD11bhi: NPM1c indel freq. 94%
F
Cas9 only
sgCD19
sgNPM1c
BrdU
S: 37%
S: 40%
S: 18%
G1: 52%
G1: 50%
G1: 73%
7-AAD
G
Gate: single cells
CD14
CD11b
BrdU
CD14HiCD11bHi
S=4%
G1=81%
CD14LoCD11bLo
S=29%
G1=62%
7-AAD

Figure S2. Nuclear relocalization of NPM1c induces cell growth arrest and differentiation in AML cell lines (Related to Figure 2).

(A) Viable cell counts by trypan blue exclusion of IMS-M2 cells transfected with Cas9 only, sgCD19 or sgNPM1c. Equal numbers of cells were plated 3 days after electroporation. Results are reported as ratio to Cas9 only control (n=3; mean ± SEM).

(B) Schematic representation of the *in vivo* experiment with OCI-AML3 cells. At the time of sacrifice, OCI-AML3 cells had predominantly engrafted the livers.

(C) Plot showing indel frequencies at target loci at time of transplant and sacrifice (sgCD19 n=2; sgCD45 and sgNPM1c n=3; mean ± SEM).

(D) Flow cytometry analysis of CD14 expression in OCI-AML3 cells 9 days after electroporation. Left panel shows distribution of CD14 signal for indicated sgRNA. Right panel shows the percentage of $CD14^{+}$ cells (n=4; mean ± SEM). The cut-off point for CD14 positivity was set at the last percentile of the gaussian curve of Cas9 only controls.

(E) Sorting strategy of differentiated ($CD14^{hi}CD11b^{hi}$) and undifferentiated ($CD14^{lo}CD11b^{lo}$) OCI-AML3 cells 10 days following electroporation with sgNPM1c (left). Sorting purity check displayed as overlay of contour plots of sorted populations (right). Indel frequencies of sorted populations are shown below.

(F) Flow cytometry dot plots showing cell cycle analysis by BrdU incorporation and 7-AAD staining in OCI-AML3 cells 9 days following transfection with sgNPM1c or controls. G1 and S phases are gated with percentages shown.

(G) Flow cytometry dot plots showing cell cycle analysis by BrdU incorporation and 7-AAD staining of differentiated ($CD14^{hi}CD11b^{hi}$) and undifferentiated ($CD14^{lo}CD11b^{lo}$) OCI-AML3 cells 9 days following transfection with sgNPM1c. G1 and S phases are gated with percentages shown.

* $p<0.05$, ** $p<0.01$, *** $p<0.001$; unpaired t-test with Welch's correction.

See also Table S2.

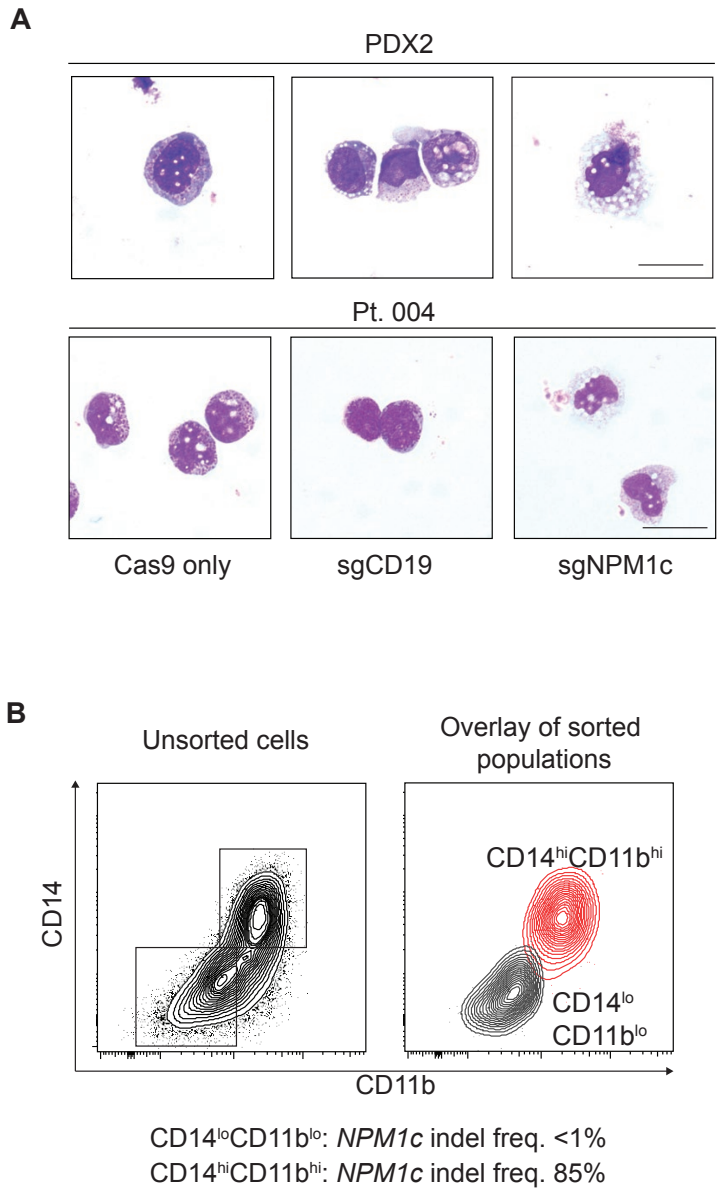

Figure S3. Nuclear relocalization of NPM1c induces differentiation of primary AML cells (Related to Figure 3).

(A) May-Grünwald Giemsa staining of PDX2 cells (top) and primary AML cells from Pt. 004 (bottom), 9 days following transfection with sgNPM1c or controls. Scale bar: 20μm.

(B) Sorting strategy of differentiated ($CD14^{hi}CD11b^{hi}$) and undifferentiated ($CD14^{lo}CD11b^{lo}$) primary AML cells (Pt. 004) 10 days following electroporation with sgNPM1c (left). Sorting purity check displayed as overlay of contour plots of sorted populations (right). Indel frequencies of sorted populations are shown below.

See also Table S4.

Table S3. Genomic features of primary AML samples (Related to Figure 3).

Patient nr.	Karyotype	*NPM1* status	Additional mutations
Pt. 001	46,XX,t(9;11)(p22;q23)[20]	WT	*NRAS* G12D, *FLT3* F594V
Pt.002	45,X,-X,+1,der(1;3)(q10;p10),t(8;21)(q22;q22)[20]	WT	*KIT* D816V
Pt.003	46,XX[18]	MutA	*DNMT3A* L504fs*147, *IDH1* R132G , *FLT3*-ITD
Pt.004	46,XX[20]	MutA	*IDH2* R140Q, *FLT3*-ITD
Pt.005	46,XX,-5,+mar[7]/46,XX,del(2)(q33)[4]/46,XX[9]	WT	*CEBPA* F106fsX54, *CEBPA* L315_E316insV, *JAK3* R149Q
Pt.006	46,XX,add(11)(p15)[17]/46,idem,add(6)(q23)[3]	MutA	*DNMT3A* S714C, *IDH2* R140Q, *FLT3*-ITD, *WT1* S381fs
Pt.009	46, XY [20]	MutA	*DNMT3A**, *CREBBP**
Pt.010	46,XX,del(9)(q13q22)[20]	MutB	*IDH2**

* Mutation not specified

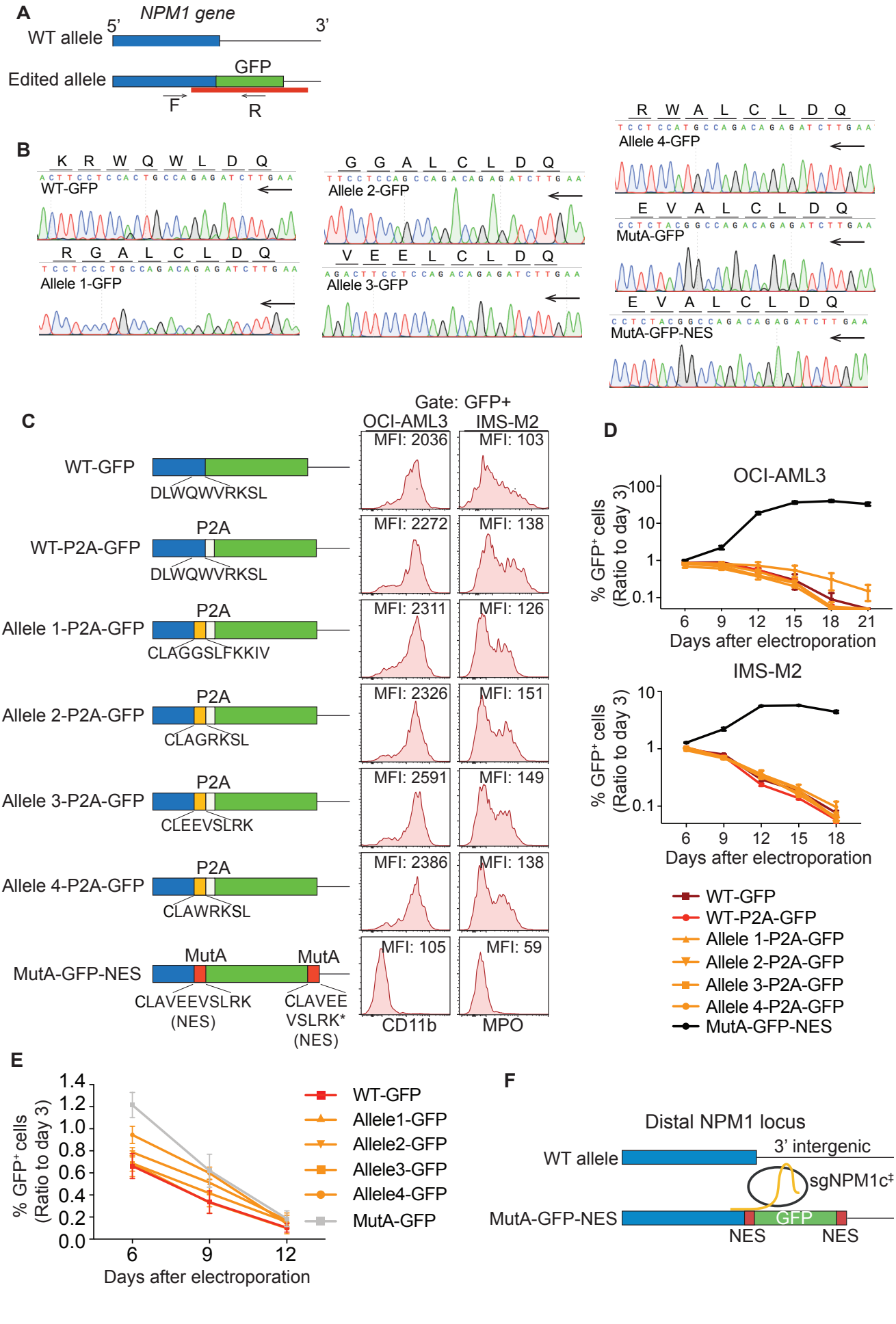
A
NPM1 gene
WT allele
5'
3'
Edited allele
GFP
F
R
B
K R W Q W L D Q
WT-GFP
G G A L C L D Q
Allele 2-GFP
R G A L C L D Q
Allele 1-GFP
V E E L C L D Q
Allele 3-GFP
R W A L C L D Q
Allele 4-GFP
E V A L C L D Q
MutA-GFP
E V A L C L D Q
MutA-GFP-NES
C
Gate: GFP+
OCI-AML3
IMS-M2
WT-GFP
DLWQWVRKSL
MFI: 2036
MFI: 103
WT-P2A-GFP
P2A
DLWQWVRKSL
MFI: 2272
MFI: 138
Allele 1-P2A-GFP
P2A
CLAGGSLFKKIV
MFI: 2311
MFI: 126
Allele 2-P2A-GFP
P2A
CLAGRKSL
MFI: 2326
MFI: 151
Allele 3-P2A-GFP
P2A
CLEEVSLRK
MFI: 2591
MFI: 149
Allele 4-P2A-GFP
P2A
CLAWRKSL
MFI: 2386
MFI: 138
MutA-GFP-NES
MutA
MutA
CLAVEEVSLRK
(NES)
CLAVEE
VSLRK*
(NES)
MFI: 105
MFI: 59
CD11b
MPO
D
OCI-AML3
% GFP+ cells
(Ratio to day 3)
100
10
1
0.1
6 9 12 15 18 21
Days after electroporation
IMS-M2
% GFP+ cells
(Ratio to day 3)
10
1
0.1
6 9 12 15 18
Days after electroporation
WT-GFP
WT-P2A-GFP
Allele 1-P2A-GFP
Allele 2-P2A-GFP
Allele 3-P2A-GFP
Allele 4-P2A-GFP
MutA-GFP-NES
E
% GFP+ cells
(Ratio to day 3)
1.4
1.2
1.0
0.8
0.6
0.4
0.2
0.0
6 9 12
Days after electroporation
WT-GFP
Allele1-GFP
Allele2-GFP
Allele3-GFP
Allele4-GFP
MutA-GFP
F
Distal NPM1 locus
WT allele
3' intergenic
sgNPM1c‡
MutA-GFP-NES
GFP
NES
NES

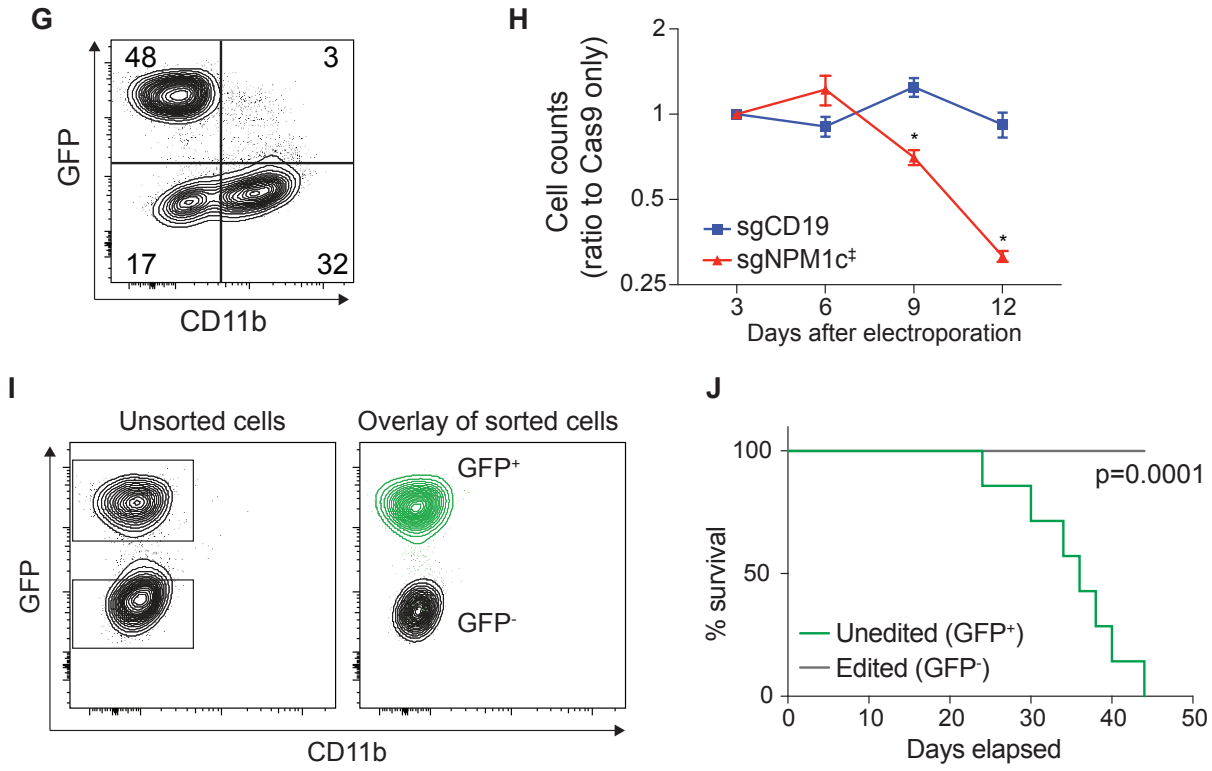

Figure S4. Leukemic phenotype of AML with mutated *NPM1* is dependent on the nuclear export of NPM1c (Related to Figure 4).

(A) Schematic representation of the strategy for genotyping precisely edited cells. The forward primer (F) anneals to a sequence outside of the HDR template (red line), while the reverse primer (R) primer anneals to the GFP sequence. Reverse primer was used for Sanger sequencing.

(B) Sanger sequencing traces of the PCR products following precise editing. Amino acid sequences are shown above. DNA sequence trace represents reverse complement of CDS.

(C) HDR templates used for precise editing of the NPM1c allele, including location of the cleavable linker P2A (left). Flow cytometry showing immunophenotypic differentiation features including CD11b (OCI-AML3) and MPO (IMS-M2) (right).

(D) Percentages of edited cells (GFP+) over 3 weeks (n=3; mean ± SEM). The cut-off point for GFP positivity was set at the last percentile of the gaussian curve of sgNPM1c only transfected cells.

(E) Data from Figure 4D are reproduced with adjusted X and Y axes to highlight differences between IMS-M2 cells edited with indicated constructs.

(F) Schematic representation of the strategy for allele-specific disruption of the MutA-GFP-NES allele in *NPM1*$^{WT/MutA\text{-}GFP\text{-}NES}$ OCI-AML3 cells.

(G) Flow cytometry contour plots showing GFP and CD11b expression in *NPM1*$^{WT/MutA\text{-}GFP\text{-}NES}$ OCI-AML3 cells 8 days following transfection with sgNPM1c‡.

(H) Viable cell counts by trypan blue exclusion of *NPM1*$^{WT/MutA\text{-}GFP\text{-}NES}$ OCI-AML3 cells transfected with Cas9 only, sgCD19 or sgNPM1c. Equal numbers of cells were plated 3 days after electroporation. Results are reported as ratio to Cas9 only control (n=3; mean ± SEM).

(I) Sorting strategy of unedited (GFP^+) and edited (GFP^+) *NPM1*$^{WT/MutA\text{-}GFP\text{-}NES}$ OCI-AML3 cells 3 days following electroporation with sgNPM1c‡ (left). Sorting purity check displayed as overlay of contour plots of sorted populations (right).

(J) Kaplan-Meier survival curves of NSG mice transplanted with unedited (GFP^-) or edited (GFP^+) *NPM1*$^{WT/MutA\text{-}GFP\text{-}NES}$ OCI-AML3 cells (n=7 for unedited, n=7 for edited; p value derived from log-rank test).

* $p<0.05$, ** $p<0.01$, *** $p<0.001$; unpaired t-test with Welch's correction.

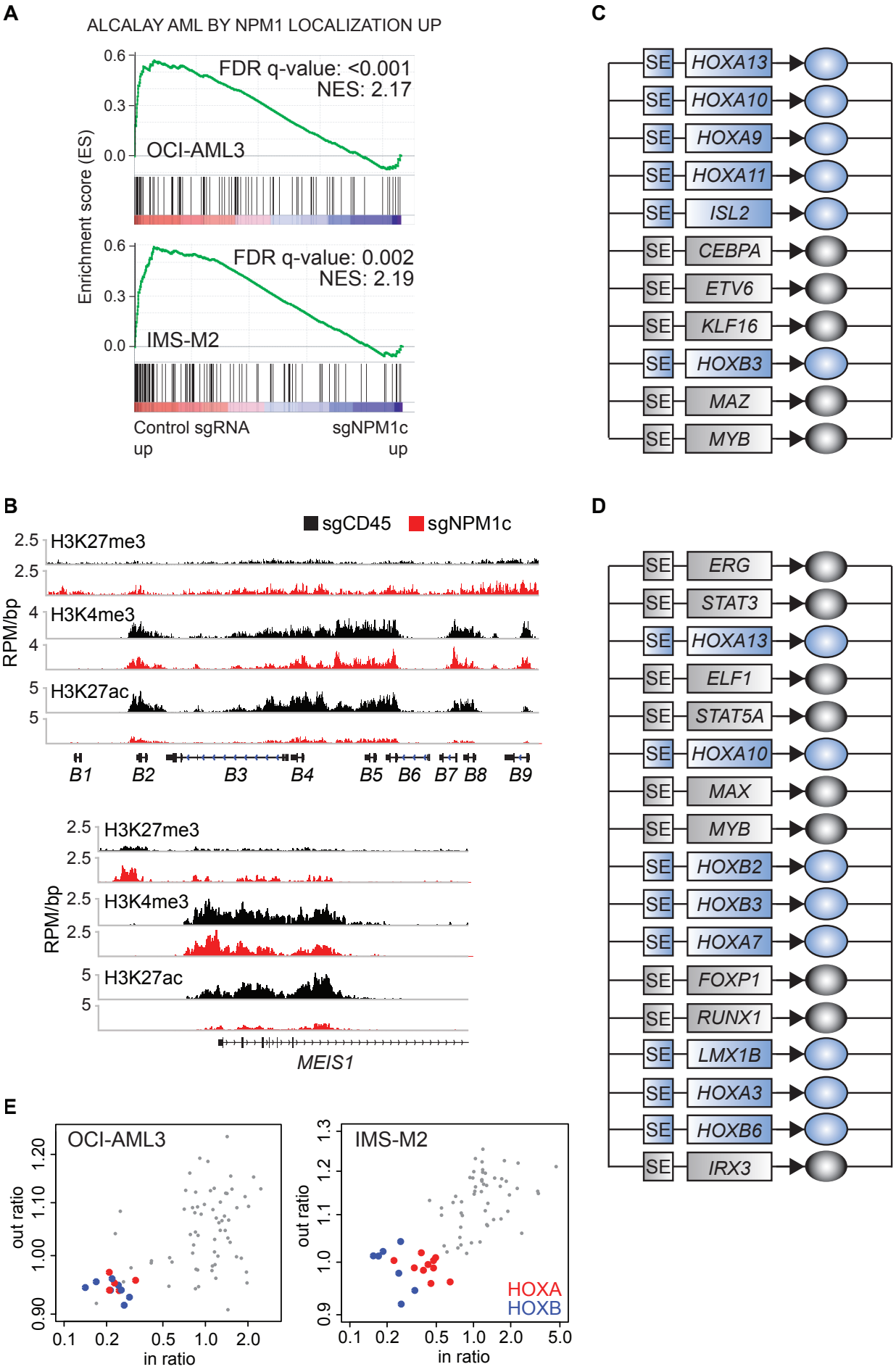
A
ALCALAY AML BY NPM1 LOCALIZATION UP
FDR q-value: <0.001
NES: 2.17
OCI-AML3
FDR q-value: 0.002
NES: 2.19
IMS-M2
Enrichment score (ES)
Control sgRNA up
sgNPM1c up
B
sgCD45
sgNPM1c
H3K27me3
H3K4me3
H3K27ac
RPM/bp
B1 B2 B3 B4 B5 B6 B7 B8 B9
MEIS1
C
SE HOXA13
SE HOXA10
SE HOXA9
SE HOXA11
SE ISL2
SE CEBPA
SE ETV6
SE KLF16
SE HOXB3
SE MAZ
SE MYB
D
SE ERG
SE STAT3
SE HOXA13
SE ELF1
SE STAT5A
SE HOXA10
SE MAX
SE MYB
SE HOXB2
SE HOXB3
SE HOXA7
SE FOXP1
SE RUNX1
SE LMX1B
SE HOXA3
SE HOXB6
SE IRX3
E
OCI-AML3
IMS-M2
out ratio
in ratio
HOXA
HOXB

Figure S5. Nuclear relocalization of NPM1c induces HOX/MEIS1 downregulation (Related to Figure 5).

(A) GSEA plot showing “upregulated genes in primary acute myeloid leukemia (AML) with mutated *NPM1*” signature in OCI-AML3 cells (top) and IMS-M2 cells (bottom) transfected with control sgRNAs versus sgNPM1c. FDR=false discovery rate; NES=normalized enrichment score.

(B) Gene track view of H3K27me3, H3K4me3, and H3K27ac ChIP-seq signal at HOXB locus (top) and *MEIS1* locus (bottom) 3 days following transfection of sgCD45 (black) or sgNPM1c (red) into OCI-AML3 cells.

(C) Core regulatory circuitry (CRC) analysis performed using H3K27ac ChIP-seq data from OCI-AML3 cells transfected with sgCD45 control. Components of the CRC with more than 50% loss of H3K27ac signal at their super-enhancer (SE) 3 days following transfection with sgNPM1c are shaded blue.

(D) Core regulatory circuitry (CRC) analysis performed using H3K27ac ChIP-seq data from IMS-M2 cells transfected with sgCD45 control. Components of the CRC with more than 50% loss of H3K27ac signal at their super-enhancer (SE) 3 days following transfection with sgNPM1c are shaded blue.

(E) Scatter-plot showing results of dynamic CRC analysis performed using H3K27ac ChIP-seq data from OCI-AML3 cells (left) and IMS-M2 cells (right) treated with sgCD45 or sgNPM1c. For each transcription factor in the network, the “in ratio” represents the change in H3K27ac signal at transcription factor binding site (TFBS) motif instances within its own enhancers (autoregulation) and the “out ratio” represents the change in H3K27ac signal at TFBP motif instances targeting enhancers for all other transcription factors in the network.

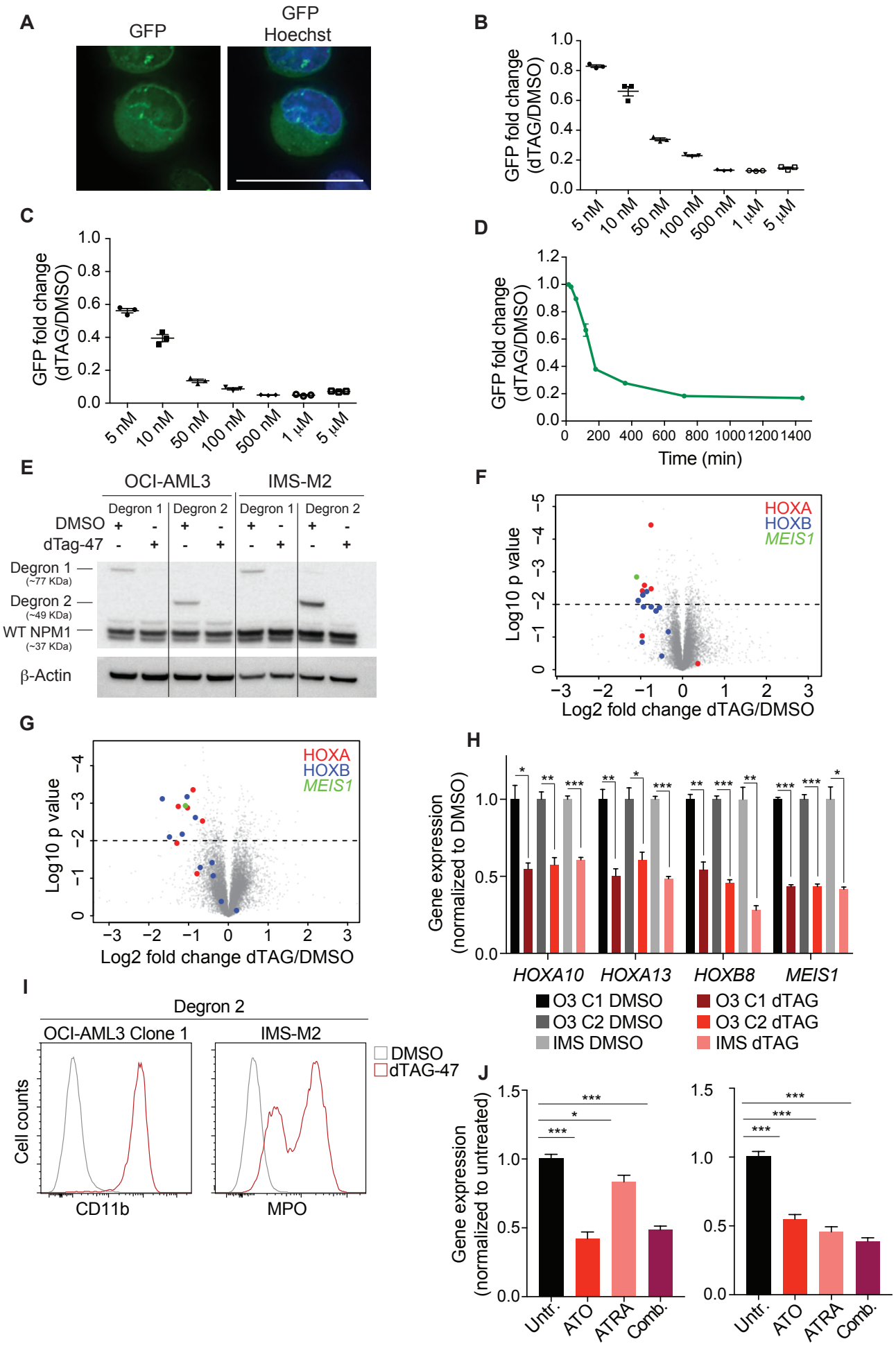
A
GFP
GFP Hoechst
B
GFP fold change (dTAG/DMSO)
5 nM
10 nM
50 nM
100 nM
500 nM
1 μM
5 μM
C
GFP fold change (dTAG/DMSO)
D
GFP fold change (dTAG/DMSO)
Time (min)
E
OCI-AML3
IMS-M2
Degron 1
Degron 2
DMSO
dTag-47
Degron 1 (~77 KDa)
Degron 2 (~49 KDa)
WT NPM1 (~37 KDa)
β-Actin
F
HOXA
HOXB
MEIS1
Log10 p value
Log2 fold change dTAG/DMSO
G
HOXA
HOXB
MEIS1
Log10 p value
Log2 fold change dTAG/DMSO
H
Gene expression (normalized to DMSO)
HOXA10
HOXA13
HOXB8
MEIS1
O3 C1 DMSO
O3 C2 DMSO
IMS DMSO
O3 C1 dTAG
O3 C2 dTAG
IMS dTAG
I
Degron 2
OCI-AML3 Clone 1
IMS-M2
DMSO
dTAG-47
Cell counts
CD11b
MPO
J
Gene expression (normalized to untreated)
Untr.
ATO
ATRA
Comb.

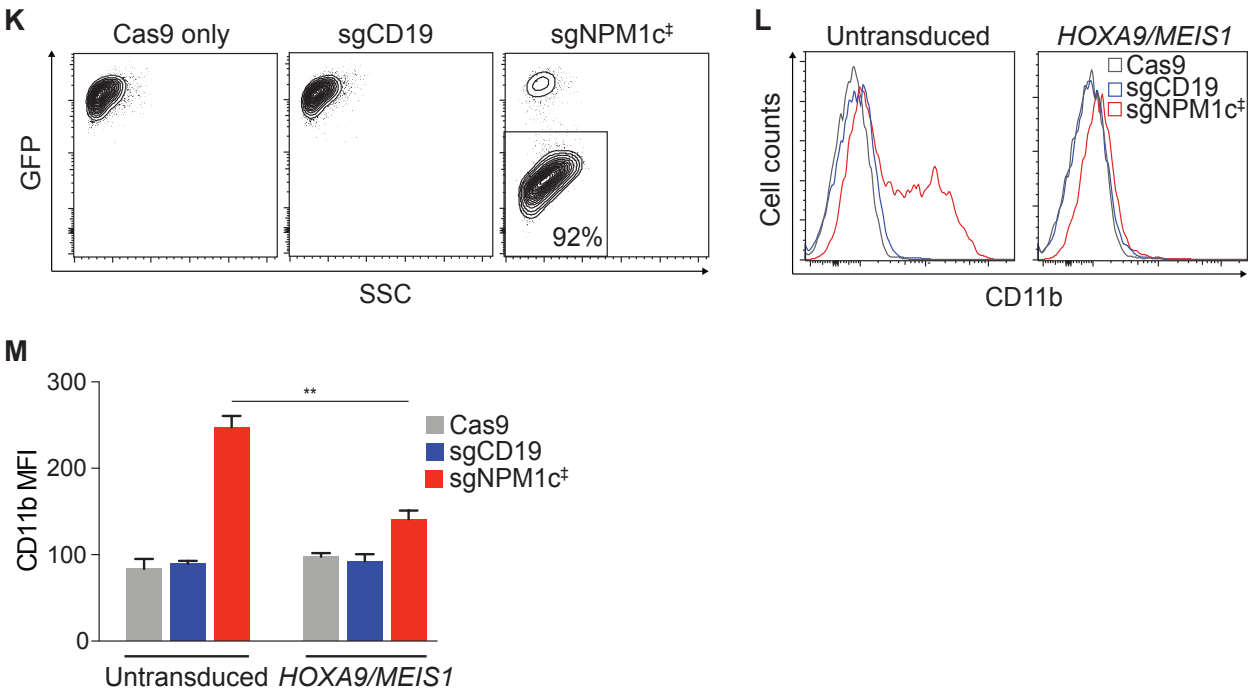

Figure S6. NPM1c maintains the leukemic state through HOX/MEIS1 expression (Related to Figure 6).

(A) Fluorescence microscopy of live OCI-AML3 *NPM1*$^{WT/Degron1}$ (Clone 2) cells. Scale bar: 25 μM.

(B) Expression fold change of the Degron 1 fusion protein upon increasing concentrations of dTAG-47 (24 hr) analyzed by flow cytometry in *NPM1*$^{WT/Degron1}$ OCI-AML3 cells (Clone 2), calculated as ratio of GFP MFI of dTAG-treated and DMSO-treated cells (n=3).

(C) Expression fold change of the Degron 1 fusion protein upon increasing concentrations of dTAG-47 (24 hr) analyzed by flow cytometry in *NPM1*$^{WT/Degron1}$ IMS-M2 (bulk) cells, calculated as ratio of GFP MFI of dTAG-treated and DMSO-treated cells (n=3).

(D) GFP expression levels of Degron 1 fusion protein over time upon 500 nM dTAG-47, analyzed by flow cytometry in *NPM1*$^{WT/Degron1}$ OCI-AML3 (Clone 1) cells and calculated as ratio of GFP MFI of dTAG-treated and DMSO-treated cells (n=3; mean ± SEM).

(E) Western blot analysis of *NPM1*$^{WT/Degron1}$ and *NPM1*$^{WT/Degron2}$ OCI-AML3 clones and IMS-M2 (bulk) cells demonstrating almost complete loss of both NPM1c fusion proteins following 24 hr treatment with 500nm dTAG-47. Higher molecular weight bands correspond to the indicated NPM1c fusion protein. Membrane was blotted with an anti N-terminal NPM1 antibody.

(F) Volcano plot showing RNA sequencing data for *NPM1*$^{WT/Degron1}$ OCI-AML3 Clone 2 cells after 6 hr treatment with 500 nM dTAG-47. Highlighted in red, blue and green are respectively HOXA, HOXB and *MEIS1* genes.

(G) Volcano plot showing RNA sequencing data for *NPM1*$^{WT/Degron1}$ IMS-M2 (bulk) cells after 6 hr treatment with 500 nM dTAG-47. Highlighted in red, blue and green are respectively HOXA, HOXB and *MEIS1* genes.

(H) qPCR data of indicated genes in *NPM1*$^{WT/Degron1}$ OCI-AML3 (Clones 1 and 2) and IMS-M2 (bulk) cells following 6 hr treatment with 500 nM dTAG-47 or DMSO (n=3; mean ± SEM).

(I) CD11b and MPO expression levels after 7 days of treatment with 500 nM dTAG-47 in *NPM1*$^{WT/Degron2}$ OCI-AML3 Clone 1 and IMS-M2 (bulk) cells.

(J) *HOXA9* qPCR data from OCI-AML3 cells treated with arsenic trioxide (ATO) and/or all-*trans* retinoic acid (ATRA) for 16 hr (left) or 48 hr (right) (n=6; mean ± SEM).

(K) GFP expression of NPM1$^{WT/MutA-GFP-NES}$ cells 9 days after transfection with an sgRNA targeting the mutant *NPM1* allele (sgNPM1c‡) or controls (Cas9 only and sgCD19). Efficient generation of indels at the C-terminus of the *NPM1c* allele results in shifting of the reading frame of the C-terminal NES and loss of GFP signal. This approach allows for gating edited cells based on GFP negativity.

(L) Histogram plots depicting CD11b expression in *NPM1*$^{WT/MutA-GFP-NES}$ OCI-AML3 cells with and without ectopic expression of *HOXA9/MEIS1* 9 days following transfection with sgNPM1c‡ and controls (Cas9 only and sgCD19). GFP negative cells were gated in both samples transfected with sgNPM1c‡, while no gate on GFP was drawn in control samples.

(M) Histograms representing the median fluorescence intensities (MFI) of CD11b in *NPM1*$^{WT/MutA-GFP-NES}$ OCI-AML3 cells 9 days following transfection with sgNPM1c‡ and controls. GFP negative cells were gated in both untransduced and *HOXA9/MEIS1*-transduced samples transfected with sgNPM1c‡, while no gate on GFP was drawn in control samples (n=3; mean ± SEM).

O3=OCI-AML3; IMS=IMS-M2; C1=Clone 1; C2=Clone 2.

* p<0.05, ** p<0.01, *** p<0.001; unpaired t-test with Welch's correction.

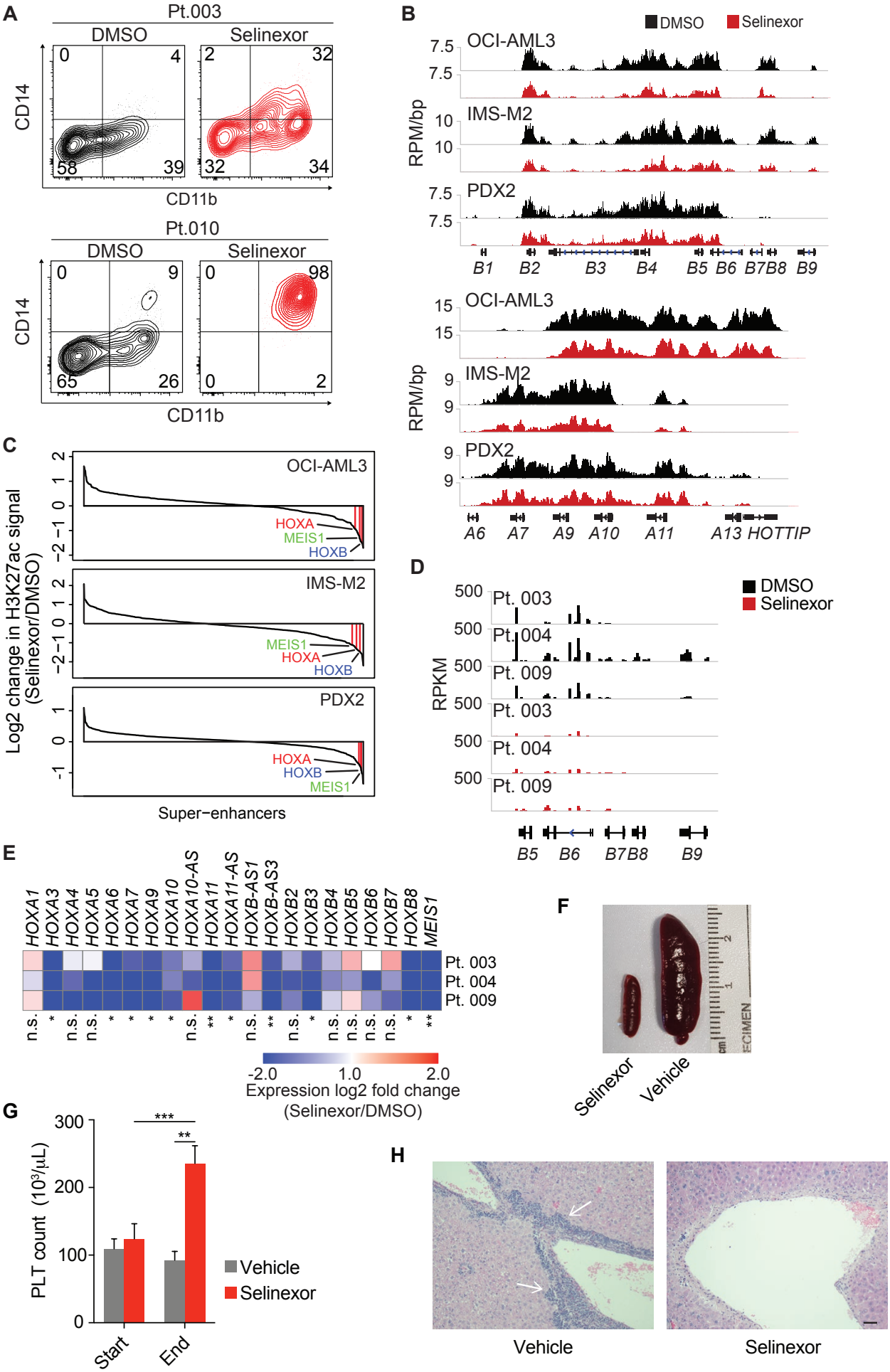
A
Pt.003
DMSO
Selinexor
CD14
CD11b
Pt.010
B
DMSO
Selinexor
OCI-AML3
IMS-M2
PDX2
RPM/bp
B1 B2 B3 B4 B5 B6 B7B8 B9
A6 A7 A9 A10 A11 A13 HOTTIP
C
Log2 change in H3K27ac signal (Selinexor/DMSO)
HOXA
MEIS1
HOXB
Super−enhancers
D
RPKM
Pt. 003
Pt. 004
Pt. 009
E
HOXA1 HOXA3 HOXA4 HOXA5 HOXA6 HOXA7 HOXA9 HOXA10 HOXA10-AS HOXA11 HOXA11-AS HOXB-AS1 HOXB-AS3 HOXB2 HOXB3 HOXB4 HOXB5 HOXB6 HOXB7 HOXB8 MEIS1
Expression log2 fold change (Selinexor/DMSO)
F
Selinexor
Vehicle
G
PLT count (10³/μL)
Vehicle
Selinexor
Start
End
H
Vehicle
Selinexor

Figure S7. XPO1 inhibition recapitulates genetic disruption of *NPM1c* nuclear export signal and has *in vivo* antileukemic activity (Related to Figure 7).

(A) Flow cytometry contour plots showing CD14 and CD11b expression in two primary AML samples (Pt. 003 and Pt. 010) after 12 days of 50 nM Selinexor or DMSO. Cells were co-cultured with HS-5 human stromal cells.

(B) Gene track view of H3K27ac ChIP-seq signal at distal HOXA locus (top) and HOXB locus (bottom) after 24 hr treatment with 100nM Selinexor or DMSO in OCI-AML3, IMS-M2 and PDX2 cells.

(C) Waterfall plot depicting change in H3K27ac ChIP-seq signal at super-enhancers after 24 hr treatment with 100nM Selinexor or DMSO in OCI-AML3, IMS-M2 and PDX2 cells.

(D) Gene track view of RNA-sequencing data showing distal HOXB locus in 3 primary AML samples treated with 100nM Selinexor or DMSO for 24 hr.

(E) Heatmap depicting log2-fold changes (Selinexor/DMSO) in gene expression at indicated loci after treatment of 3 primary leukemia samples with 100nM Selinexor or DMSO for 24 hr.

(F) Spleens of two representative mice treated with Selinexor (left) or vehicle (right) collected at the time of the last administration.

(G) Platelet (PLT) counts measured at the time of the first (start) and last (end) administration in mice treated with Selinexor or vehicle (n=14 for vehicle, n=17 for Selinexor; mean ± SEM).

(H) Histology of the livers of two representative mice treated with vehicle (left) or Selinexor (right), performed at the time of the last administration. Scale bar 100 μm. White arrows indicate leukemic infiltrates.

* $p<0.05$, ** $p<0.01$, *** $p<0.001$; two-tailed ratio t-test.